A THEORETICAL PRESSURE-DRIVEN RESPONSE FUNCTION FOR COMPOSITE SOLID PROPELLANTS

B. M. Rasmussen, R. A. Frederick, and M. D. Moser
The University of Alabama in Huntsville
Huntsville, AL

G. Lengellé
Office Nationale d'Etudes et de Recherches Aérospatiales (ONERA)
Palaiseau, France

ABSTRACT

The paper is a theoretical study of composite solid propellant combustion. Specifically, it contains models of AP/HTPB deflagration, with predictions of both steady-state ballistics and pressure-coupled frequency response for single-AP-particle-diameter (mono-modal) propellants. The steady-state model is a system of eight equations derived from physical principles, and the nonsteady model is a repetition of the steady equations, with some additional terms to account for "capacitance" in the solid phase. Steady-state predictions agree with experimental data for both burning rate and σ_p. Nonsteady results are discouraging, because the temperature profile in the solid phase seems to be reacting too swiftly to changes in pressure. The problem may require a re-formulation in order to remove some of the computational difficulties.

INTRODUCTION

REVIEW

Composite propellant combustion is a very complicated phenomenon that does not yield easily to pure analytical approaches. One of the first true composite steady-state models was the Beckstead-Derr-Price (BDP) multiple flame model[1], introduced in 1970. It inspired many similar models and improvements[2], and most composite models today still follow the same basic example. Some notable improvements have been inclusion of separate surface temperatures for binder and oxidizer[3,4], and new techniques for modeling multi-modal propellants[5] (i.e. different AP particle diameters in the same propellant).

While such models have become better at predicting steady-state properties, there has been some difficulty extending the heterogeneous framework to nonsteady models[6]. Most nonsteady models since the 1950's have relied on Quasi-Steady gas phase, Homogeneous solid phase, One-Dimensional (QSHOD) assumptions. The assumption of a homogeneous solid phase, in particular, greatly simplifies the final form of the response function, so the heterogeneity of composite propellants makes them poor subjects for QSHOD models.

There have been several approaches to accounting for heterogeneity in nonsteady models[6]. One tactic is to use a steady-state model to calculate physical parameters, which in turn plug into QSHOD models[7,8]. Another approach is to perturb and linearize a steady-state model.

This work was performed under contract number N00014-96-1-1182 with the Office of Naval Research and contract number PC184577 with the California Institute of Technology.

The study presented here is a different approach based on direct simulation. The first part of the study is a steady-state model that seems to predicts reasonable burning rate vs. pressure curves. The second part is an nonsteady model based on the steady-state description. The nonsteady model is almost identical to the steady-state model, but it does include some additional terms to account for thermal lags and conductive "capacitance" in the solid phase. Simpler versions of this method for heterogeneous propellants have created reasonable non-linear response predictions[9].

A previous attempt along these lines was unsuccessful, mostly due to an inability of the steady-state model to accurately predict initial temperature sensitivity[10],[11]. The current study has produced better steady-state results, although nonsteady results have not been adequate.

STEADY-STATE MODEL DEVELOPMENT

The steady-state model is a separate-surface-temperature model with a heterogeneous flame structure similar to the original BDP proposition. It is a model of mono-modal AP/HTPB propellants only, although the techniques used here should extend directly to multi-modal propellants with other oxidizers and inert binders. It is a system of eight equations, with eight dependent variables:

- Total mass flux
- Oxidizer mass flux
- Binder mass flux
- Height of pre-mixed (AP) flame
- Height of total flame
- Surface temperature of binder
- Surface temperature of oxidizer
- Pre-mixed flame temperature

Figure 1 is a sketch of the surface of the propellant. As in the BDP model, there are three flames. The *pre-mixed AP flame* represents pure AP deflagration, which is an exothermic decomposition into perchloric acid and ammonium. The *reaction flame* is a kinetics-dominated flame of binder decomposition products reacting with perchloric acid. Both AP and binder residuals decompose into the final combustion products in the *diffusion flame*.

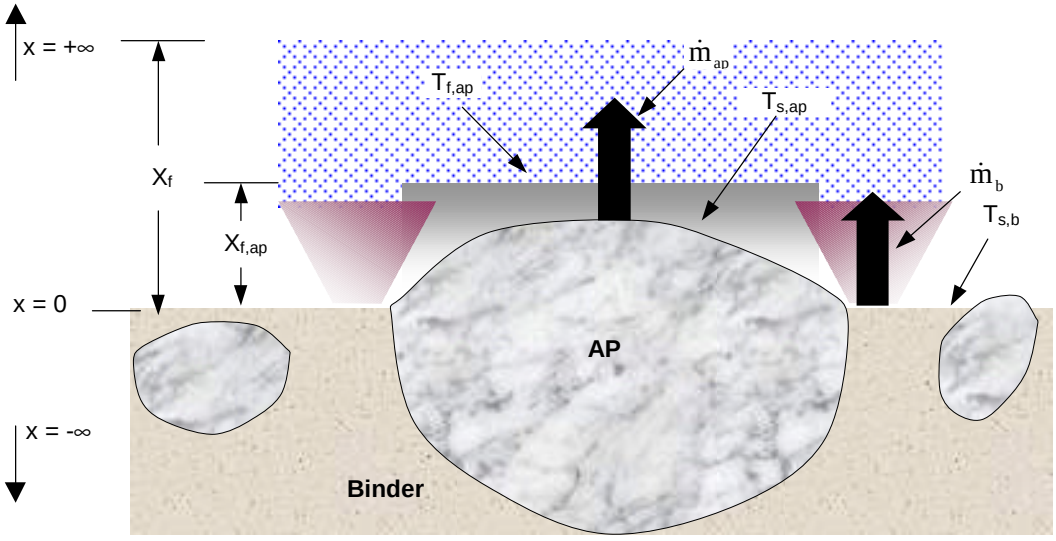

Figure 1: Conceptual Picture

The equations that comprise the steady-state model are below. In the interest of brevity, they have short descriptions and a non-rigorous derivation. The one-dimensional coordinate system is defined as 0 at the surface, +∞ high above the surface, and -∞ far below the surface. (See Figure 1.)

The mass fluxes of the binder and oxidizer are Arrhenius expressions. Some researchers have raised questions about the applicability of simple Arrhenius pyrolysis relationships to time-dependent systems[12], but the following expressions are probably adequate for the time being:

Oxidizer:

$$\dot{m}_{ap} = A_{s,ap} \exp\left(-\frac{E_{s,ap}}{RT_{s,ap}} \right) \tag{1}$$

Binder[13]:

$$\dot{m}_{b} = A_{s,b} \exp\left(-\frac{E_{s,b}}{RT_{s,b}} \right) \tag{2}$$

The mass flux of the propellant is an algebraic combination of the mass fluxes of the binder and oxidizer. It is based on a "column" assumption of linear burning.

$$m_{p} = \alpha_{ap} \frac{\rho_{p}}{\rho_{ap}} \dot{m}_{ap} + (1-\alpha_{ap}) \frac{\rho_{p}}{\rho_{b}} m_{b} \tag{3}$$

The pre-mixed AP flame is a second-order kinetics-dominated flame, so it is related to the inverse square of the pressure.

$$x_{f,ap} = \frac{\dot{m}_{ap}}{P^{2} A_{g,ap} \exp\left(-\frac{E_{g,ap}}{RT_{f,ap}} \right)} \tag{4}$$

The expression for total flame height is somewhat more complicated. It too has a reaction component that is related to the inverse square of the pressure.

$$x_{r} = \frac{\dot{m}_{p}}{P^{2} A_{r} \exp\left(-\frac{E_{r}}{RT_{f}} \right)} \tag{5}$$

Diffusion flame height comes from a common relationship.

$$x_{d} = \frac{\dot{m}_{p} D_{ap}^{*\,2}}{A_{diff} \left(\rho_{g} D_{g} \right)_{eff}} \tag{6}$$

D^*_{ap} is a *characteristic* AP particle diameter, related to the mass fluxes of AP and total propellant and the initial AP diameter.

$$D_{ap}^{*} = \frac{2D_{ap}}{\sqrt{6\frac{\rho_p \dot{m}_{ap}}{\rho_{ap} \dot{m}_p}}} \tag{7}$$

Two effects contribute to the value of the diffusion coefficient. The dominant contribution is ordinary laminar diffusion mixing, which is itself related to a reference diffusion coefficient and temperature[14].

$$\left(\rho_g D_g\right)_{lam} = \rho_g D_0 \frac{T_{f,ap}^{\ \beta}}{P} = D_0 T_{f,ap}^{\ \beta-1} \frac{M}{R} \qquad \text{where } \beta = 1.75 \tag{8}$$

As the reaction flame becomes small relative to the diffusion flame, turbulent mixing in the diffusion flame becomes significant. The following relationship is an attempt to incorporate turbulent mixing into the model:

$$\left(\rho_g D_g\right)_{turb} = K\dot{m}_p D_{ap}^{*}\left(\tan^{-1}\left(C_1 C_2\right) + \tan^{-1}\left[C_2\left(\frac{1}{x_r} - C_1\right)\right]\right) \tag{9}$$

In the above equation, K is a generic constant, close to 1, and the arctangent function is a relatively simple way to model the onset of turbulence. When the reaction height is large, turbulent mixing is negligible. As the reaction flame approaches the surface, combustion products in the diffusion flame travel a longer distance before mixing, so turbulence becomes more of a factor. Thus, C_1 controls the onset of turbulence, and C_2 controls the length of the transitional region. Figure 2 is a chart of an example arctangent function compared to reaction height.

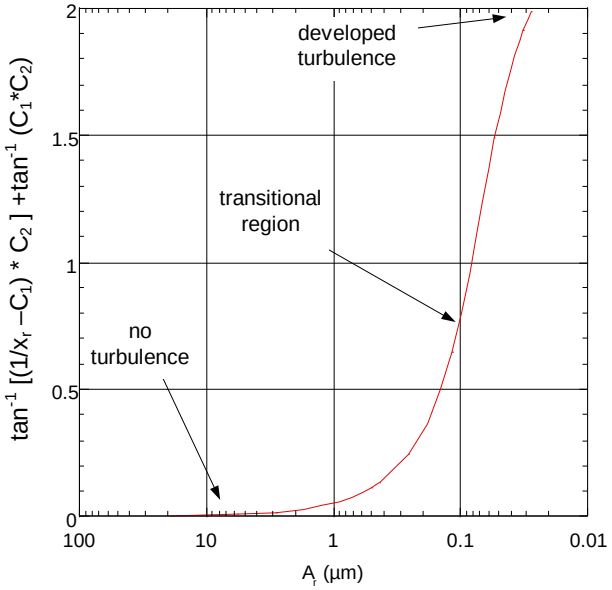

Figure 2: Onset of Turbulence as Reaction Height Falls

The expression for total flame height is therefore a combination of equations (5) - (9):

$$x_f = \frac{\dot{m}_p D_{ap}^{*\,2}}{A_{diff}\left[D_0 T_{f,ap}^{\beta-1}\frac{M}{R} + K\dot{m}_p D_{ap}^{*}\left(\tan^{-1}(C_1 C_2) + \tan^{-1}\left[C_2\left(\frac{1}{x_r} - C_1\right)\right]\right)\right]} + \frac{\dot{m}_p}{P^2 A_r \exp\left(-\frac{E_r}{RT_f}\right)} \qquad (10)$$

The oxidizer and binder have separate surface temperatures in the model. Energy balances from far below the surface (x = -8) to just above the surface (x = 0^+) provide equations for the surface temperatures of the AP and binder. The energy balance in the AP is the following (based on pure conduction into the surface):

$$\dot{m}_{ap} C_{p,or,ap} T_i + \lambda_{g,ap}\left.\frac{\partial T}{\partial x}\right|_{x=0^+} + \dot{m}_{ap} Q_{v,ap} = \dot{m}_{ap} C_{p,g,ap} T_{s,ap} + \int_{-\infty}^{0} \rho C_p \frac{\partial T}{\partial t}\partial x \qquad (11)$$

First, notice that at steady-state the integral term is zero. This is not true in the nonsteady model, however, and in fact the integral represents the thermal lag, which contributes heavily to the frequency response. (Readers familiar with combustion modeling will recognize equation (11) as a once-integrated form of the "transient heat conduction equation".)

Second, notice that one must know the shape of the temperature profile above the surface in order to calculate the partial derivative in the heat conduction term. Assume an exponential profile.

$$T(x) = (T_{s,ap} - T_{f,ap})\exp\left(-\nu\frac{x}{x_{ap}}\right) + T_{f,ap} \qquad (12)$$

ν is just a constant that relates how quickly the temperature rises to the flame height above the surface. In this study, it is assumed to be 3, since the equation will then bring the temperature to within $(1/e^3)*(T_{s,ap} - T_{f,ap})$ of the AP flame temperature at height $x = x_{ap}$. The assumed profile now leads to a solution of the conduction term and subsequently to an algebraic solution for $T_{s,ap}$.

$$\left.\frac{\partial T}{\partial x}\right|_{x=0^+} = -\frac{\nu_{ap}}{x_{ap}}(T_{s,ap} - T_{f,ap}) \qquad (13)$$

$$T_{s,ap} = \frac{\dot{m}_{ap} C_{p,or,ap} T_i + \lambda_{g,ap} T_{f,ap}\frac{\nu}{x_{f,ap}} + \dot{m}_{ap} Q_{v,ap}}{\dot{m}_{ap} C_{p,g,ap} + \lambda_{g,ap}\frac{\nu}{x_{f,ap}}} \qquad (14)$$

Proceeding with an almost identical method, the expression for surface temperature of binder is

$$T_{s,b} = \frac{\dot{m}_b C_{p,c,b} T_i + \lambda_{g,b} T_f \frac{\nu}{x_f} + \dot{m}_b Q_{v,b}}{\dot{m}_b C_{p,g,b} + \lambda_{g,ap}\frac{\nu}{x_f}} \qquad (15)$$

Another energy balance, from x_{ap} to x_f, defines the temperature of the pre-mixed flame. This energy balance does not include the integral (nonsteady) term, because the gas phase is quasi-steady by assumption. The final form of the equation for the AP flame temperature is

$$T_{f,ap} = \frac{T_f\left[\dot{m}_p C_{p,g,p} + \frac{\nu\lambda_{g,p}}{x_f - x_{f,ap}}\right] - \dot{m}_p Q_f}{\dot{m}_p C_{p,g,p} + \frac{\nu\lambda_{g,p}}{x_f - x_{f,ap}}} \tag{16}$$

In sum, the steady-state model has eight equations with six "floating parameters," which are adjusted to fit experimental data. The floating parameters are K, C_1, C_2, A_{diff}, A_r, and $A_{g,ap}$. The first three parameters define the turbulent onset (the shape of the curve in Figure 2), so they effectively constitute one floating parameter. That is, the model really has four floating parameters- A_{diff}, A_r, $A_{g,ap}$, and the shape of the turbulent mixing transition.

RESPONSE FUNCTION DEVELOMENT

The model contains two nonsteady terms; one is in integral form in equation (11), and the other, an almost identical term, is in the energy balance for the binder (not shown). Consider the ammonium perchlorate as an example. The integral term in the AP is

$$\int_0^{-\infty} \rho_{s,ap} C_{p,s,ap} \frac{\partial T(t,x)}{\partial t} dx \tag{17}$$

Thus, what is needed is an expression for $\frac{\partial T(t,x)}{\partial t}$. Start with the familiar transient heat conduction equation. (In fact, notice that the energy balance in equation (11) is really just a once-integrated version of the transient heat conduction equation with boundary values applied.)

$$\rho_{s,ap} C_{p,s,ap} \frac{\partial T}{\partial t} + \dot{m}_{ap} C_{p,s,ap} \frac{\partial T}{\partial x} - \lambda_{s,ap} \frac{\partial^2 T}{\partial x^2} = 0 \tag{18}$$

Considering just the nonsteady part leads to the following solution for T(x) at steady-state:

$$\overline{T}(x) = T_i + \left(\overline{T}_{s,ap} - T_i\right)\exp\left(\frac{x C_{p,s,ap} \overline{\dot{m}}_{ap}}{\lambda_{s,ap}}\right) \tag{19}$$

Equation (19) is necessary to provide an initial condition. The nonsteady temperature (from equation (18)) is

$$\frac{\partial T}{\partial t} = \frac{1}{\rho_{s,ap}}\left(\frac{\partial^2 T}{\partial x^2}\frac{\lambda}{C_{p,s,ap}} - \dot{m}_{ap}\frac{\partial T}{\partial x}\right) \tag{20}$$

Hence it is possible to calculate the integral in equation (17) using numerical approximations of the derivatives in (20) and progressing through iterative solutions of the model. Similarly, it is possible to calculate the integral corresponding integral term for the binder concurrently through the same method.

RESULTS AND DISCUSSION

STEADY-STATE RESULTS

Figure 3 is a plot of burning rate vs. pressure. It shows the steady-state model predictions as compared to experimental data for two mono-modal propellants- 90µm and 5µm. It also shows a theoretical prediction for a mono-modal 200µm propellant. All experimental data are for 80% AP 20% HTPB at initial temperature 298K[11].

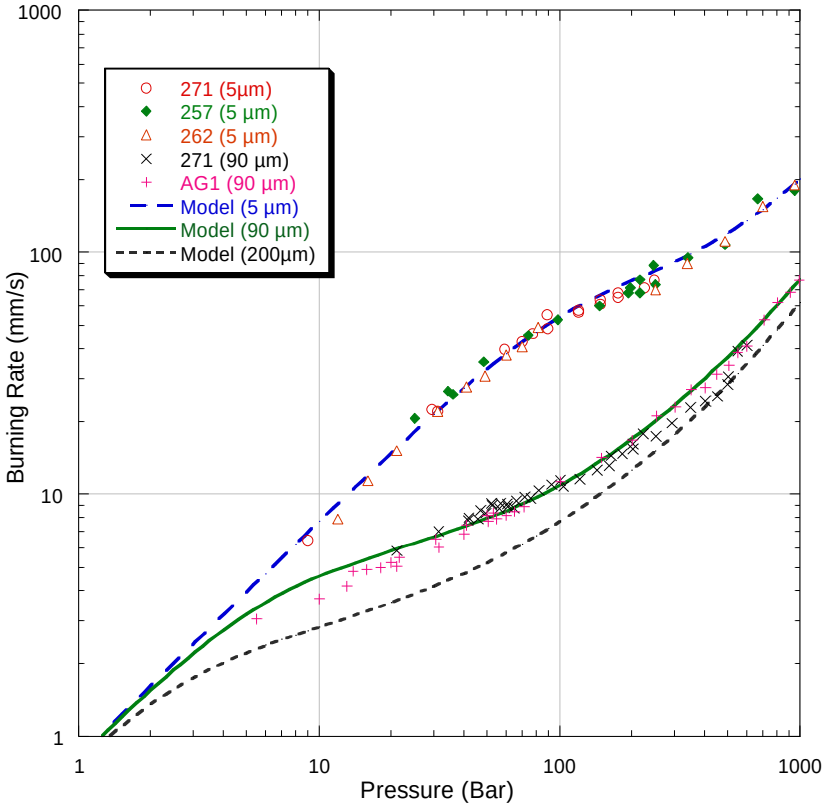

Figure 3: Steady-State Burning Rate vs. Pressure

Figure 4 is a plot of theoretical temperature sensitivity (σ_P in K^{-1}) as a function of pressure. It contains curves for 5µm, 90µm, and 200µm propellant with 80% AP, 20% HTPB. The curves come from steady-state calculations at 219K and 333K initial temperature.

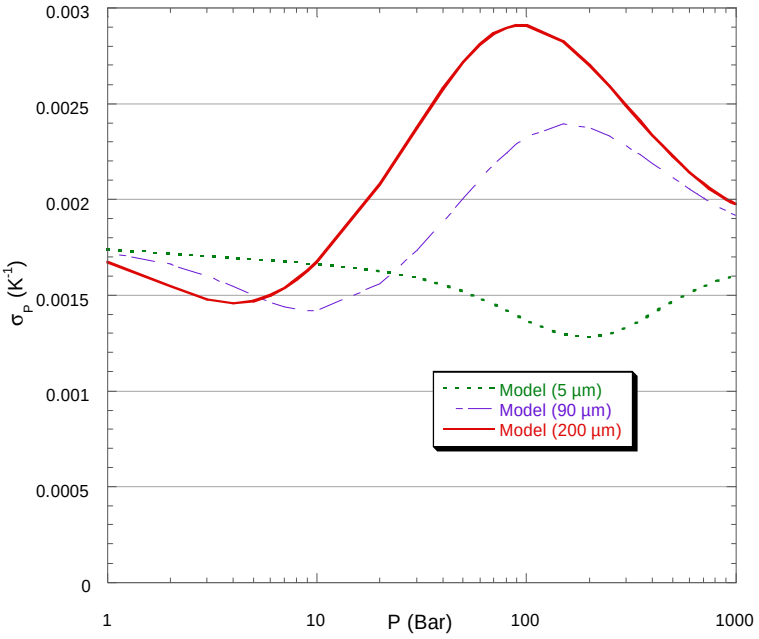

Figure 4: Initial Temperature Sensitivity Predictions

NONSTEADY RESULTS

Figure 5 shows how the system reacts to a step input. The general shape of the curve is correct for a dynamic system, but unfortunately the response time is too small. A response curve generated with this system would stay flat-lined at the pressure exponent.

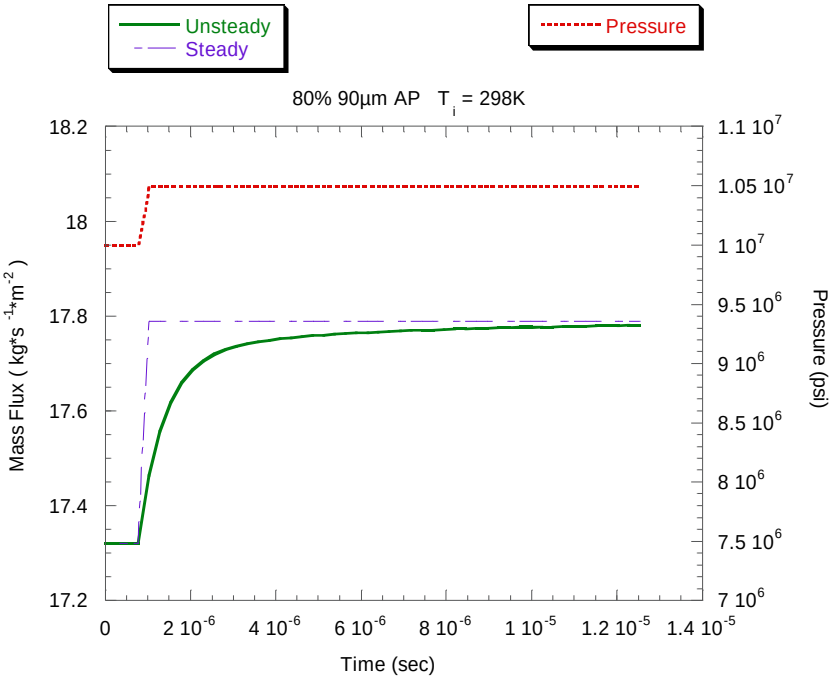

Figure 5: Nonsteady Reaction to Step Input

SUMMARY AND CONCLUSIONS

STEADY-STATE

The model does agree very closely with steady-state burning rate vs. pressure data. Less clear is the theoretical prediction of σ_p. The model predicted a range of about 0.0013 to about 0.0028 K^{-1}, which is reasonable for AP/HTPB non-aluminized propellants[15]. Further temperature sensitivity testing will be necessary in order to confirm or refute the predicted trends of σ_p as a function of pressure.

NONSTEADY

Unfortunately, the nonsteady simulation did not generate realistic response times for an AP/HTPB propellant. The expected response time for a monopropellant should be the following:

$$\tau = \frac{\alpha}{\dot{r}^2} \tag{21}$$

Equation (21) is generally on the order of milliseconds for AP/HTPB propellants, not the microseconds observed in Figure 5. Clearly, the temperature profile in the solid phase is reacting too quickly to pressure changes.

The direct simulation method itself is probably valid, however, since it has worked well for propellants that are assumed to be homogeneous[9]. Extra complications brought on by considering heterogeneous effects definitely make the formulation more difficult, but the benefits of increased understanding and a more realistic physical picture make the difficulty worthwhile. Eventually, this highly nonlinear, complex model should produce better frequency response predictions than those of current models.

NOMENCLATURE

A : pre-exponential factor
A_{diff} : diffusion constant
C : constant
C_P : constant-pressure specific heat
D : diffusion coefficient
D : AP particle diameter
E : activation energy
K : diffusion constant
M : molecular weight
$\dot{m}$: mass flux
P : pressure
Q : specific energy release (+ exothermic)
R : universal gas constant
r : burning rate
T : temperature
t : time
x : distance

α : oxidizer mass fraction, or thermal diffusivity
β : exponential diffusion constant
λ : thermal conductivity
ν : exponential growth factor
ρ : density
σ_p : initial temperature sensitivity
τ : response time

$_{ap}$: ammonium perchlorate
$_{cu}$: cubic
$_{b}$: binder
$_{c}$: condensed phase
$_{f}$: flame
$_{g}$: gas-phase
$_{i}$: initial conditions
$_{or}$: orthorhombic
$_{p}$: propellant
$_{s}$: surface
$_{v}$: vaporization
$\overline{\ }$: steady-state
$'$: differential
$_{0}$: initial

REFERENCES

[1] Beckstead, M.W., Derr, R. L., and Price, C.F. "A Model of Composite Solid-Propellant Combustion Based on Multiple Flames" *AIAA Journal* Vol. 8, Dec 1970, pp.2200-22078.

[2] Cohen, N.S. "Review of Composite Propellant Burn Rate Modeling" *AIAA Journal* Vol. 18 March, 1980. P.277-293.

[3] Beckstead, M.W., "A Model for Solid Propellant Combustion" *Eighteenth Symposium (International) on Combustion*. The Combustion Institute , Pittsburgh, PA, 1981, pp. 175-185.

[4] Cohen, N. S., and Strand, L. D., "An Improved Model for the Combustion of AP Composite Propellants" *AIAA Journal*, Vol. 20 No. 12 December, 1982, pp. 1739-1746.

[5] Renie, J. P., Condon, J. A., and Osborn, J. R. "Oxidizer Size Distribution Effects on Propellant Combustion" *AIAA Journal* August, 1979, pp. 877-883.

[6] Cohen, N. S. "Response Function Theories That Account for Size Distribution Effects— A Review" *AIAA Journal* Vol. 19 No. 7 July, 1981. pp. 907-912.

[7] Beckstead, M. W., "Combustion Calculations for Composite Solid Propellants" *13th JANNAF Combustion Meeting*, CPIA Publication 281, Vol. II, 1976, pp.299-312.

[8] Condon, J. A., Osborn, J. R., and Glick, R. L., "Statistical Analysis of Polydisperse, Heterogeneous Propellant Combustion" *13th JANNAF Combustion Meeting*, CPIA Publication 281, Vol. II, 1976, pp. 209-223.

[9] Galfetti, L., Riva, G., and Bruno, C. "Numerical Computations of Solid-Propellant Nonsteady Burning in Open or Confined Volumes," *Nonsteady Burning and Combustion Instability of Solid Propellants*, Deluca, L., Price, E. and Summerfield, M. ed. AIAA Progress in Astronautics and Aeronautics, Vol. 143, 1992 pp. 643-687.

[10] Rasmussen, B., Frederick, R., and Lengellé, G., "Pressure Coupled Frequency Response Functions of Solid Propellants" *Proceedings of the 34th JANNAF Combustion Subcommittee Meeting*, CPIA Publication 662, Vol. 2, October, 1997, pp. 263-274.

[11] Bellec, R. Duterque, J., and Lengellé, G. "Modélisation de la combustion des propergols solides aluminisés" ONERA technical report # RT 37/7128 EN Nov. 1996, pp. 54-55.

[12] Brewster, Q. and Son, S. F., "Quasi-Steady Combustion Modeling of Homogeneous Solid Propellants" *Combustion and Flame* 103, 1995, pp.11-26.

[13] Chiaverini, M. J., Harting G. C., Lu, Y.-C., Kuo, K. K., Pertez, A., Jones, S. Wygle, B, and Arves, J. P. "Pyrolysis Behavior of Hybrid Solid Fuels Under Rapid Heating Conditions" AIAA 97-3078. July, 1997.

[14] Penner, S. S., *Chemistry Problems in Jet Propulsion*, Pergammon Press, Los Angeles, 1957, p. 246.

[15] Cohen, N. S., and Flanigan, D. A. "A Literature Review of Solid Propellant Burn Rate Temperature Sensitivity" AFRPL-TR-83-042, Morton Thiokol Corporation, Huntsville, AL, October, 1983, p. 42.